Chapter 6
Cold Spray Additive Manufacture and Component Restoration

Shuo Yin, Barry Aldwell, and Rocco Lupoi

6.1 Introduction

Cold spray as an emerging coating technology was developed in the 1980s. Differing from the conventional thermal spray coating techniques, the formation of cold spray coating relies largely on the particle velocity prior to the impact rather than the temperature. Thereby, the feedstock used for cold spray remains solid state during the entire deposition process. The inevitable defects commonly encountered in the high-temperature deposition processes, e.g., oxidation, thermal residual stress, and phase transformation, can be avoided. Therefore, cold spray coatings have been widely applied in a broad range of industries including aerospace, automotive, energy, medical, marine, and other important fields, providing effective protection against high temperature, corrosion, erosion, oxidation, chemicals, etc. (Champagne and Helfritch 2016, Papyrin 2001; Vilardell et al. 2015). Apart from the aforementioned features, the thickness of cold spray coating almost has no limitation for most metals and metal matrix composites, e.g., the diamond-reinforced metal matrix composites as shown in Fig. 6.1(Yin et al. 2017). Considering this fact, cold spray has been successfully applied as an additive manufacturing technology to fabricate individual components and restore damaged components in recent years (Blose et al. 2006; Champagne et al. 2008). This development shines a new light on the conventional additive manufacturing technologies and significantly broadens application fields of cold spray.

Cold spray additive manufacturing (CSAM) as a new member of additive manufacturing family has great potentials to fabricate components with rotational structures, e.g., cylinder walls and flanges. It also allows for the production of near net-shape structures or complex geometry structures by the aid of well-designed

S. Yin (✉) • B. Aldwell • R. Lupoi
Trinity College Dublin, The University of Dublin, Department of Mechanical and Manufacturing Engineering, Parsons Building, Dublin 2, Ireland
e-mail: yins@tcd.ie; lupoir@tcd.ie

P. Cavaliere (ed.), *Cold-Spray Coatings*,
https://doi.org/10.1007/978-3-319-67183-3_6

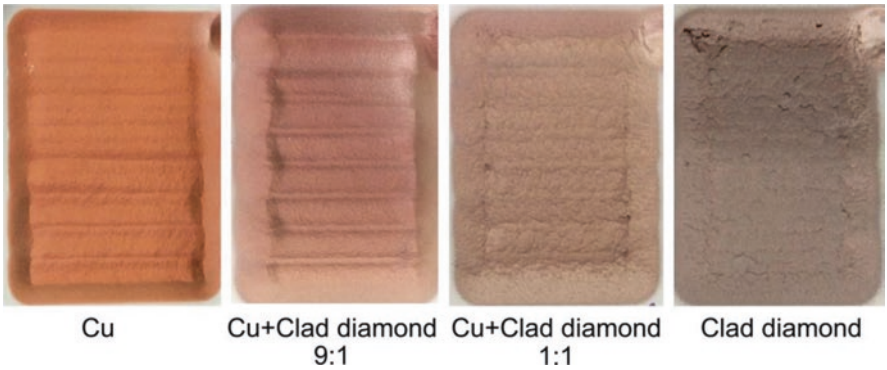

Fig. 6.1 Digital photos of thick Cu + diamond metal matrix composite coatings fabricated via cold spray (Yin et al. 2017)

masks or molds. Similar to the cold spray functional coatings, components fabricated via CSAM have superior advantages, e.g., high adhesive strength, low oxidation, and no phase transformation. Despite having many unique merits, CSAM also has obvious shortcomings. As a process which was originally developed for coating fabrication, the additive materials used for CSAM must be built on a substrate. The as-fabricated CSAM produces, therefore, consist of two parts, i.e., inner base substrate and outer new structure. This unique structure may be favorable to certain special applications, e.g., building a structure on an unweldable base materials. However, in other circumstances, the substrate may have to be removed, which increases the manufacturing cost and time. Moreover, the dimensions and surface condition of the as-fabricated CSAM components are not precise; hence, post-machining is strictly required to finalize the fabrication.

Component damage frequently occurs in service due to corrosion, wear, fatigue, or other causes. Many of the damaged components cannot be reclaimed and have to be replaced due to the lack of effective restoration methods. Cold spray as a cost-effective process has shown great potential in the repair of damaged components because of the capability to prevent adverse influence on the underlying substrate materials and unique merit to retain the feedstock's original properties. During the past decade, cold spray restoration (CSR) as a promising approach has been successfully applied to repair a variety of corroded and damaged components in various fields. The restored components are in good serviceable conditions, significantly reducing the cost by replacing a new component. Similar to other restoration techniques, cold spray feedstock cannot be deposited on the damaged component directly because the complex surface topography and unclean surface on the damaged area may adversely affect the restoration quality. Pre-machining on the damaged zone as a preparation is necessary. By preparing the damaged area, a clean and smooth surface applicable for the further cold spray filling work can be achieved. After material deposition, the as-coated components also have to be post-machined to their original dimensions. The standard CSR process normally includes the

following four stages: pre-machining on the damaged part, coating deposition, post-machining on the backfilling coating, and performance test.

While cold spray for additive manufacturing and repair applications is still an emerging technology, a large amount of research work has been carried out by both the scientific and industrial communities. Existing works mainly focused on applications, product properties, processing parameters optimization, spray strategy, and robot control. So far, a systematic summarization and review on these topics is still lacking. Therefore, in this chapter, the existing CSAM and CSR works were summarized and reviewed for the purpose of systematically introducing the progress of CSAM and CSR techniques.

6.2 Cold Spray Additive Manufacturing Applications

6.2.1 Rotational Structure Fabrication

A broad range of components have a rotational symmetry (e.g., cylinder inner and outer walls and flanges), playing significant roles in the modern industry. CSAM has great capability to fabricate components with such rotational structure. Using an external motor-drive axis to hold the mandrel substrate, the rotational structure can be easily fabricated through a simple definition of nozzle movement. Figure 6.2a shows a photo of the CSAM system located in the cold spray lab of Trinity College Dublin (TCD). The system consists of a conventional homemade cold spray system and a rotational fourth axis which is fixed on a three-axis CNC platform. It has been used for fabricating a variety of rotational structure components since its setup. For instance, an aluminum flange structure was successfully fabricated for an Irish company by this system. This flange shows features which have been manufactured using turning and drilling, including a chamfer which crosses the interface between the substrate and cold spray deposit. This demonstrates the ability to achieve a good surface finish and dimensional accuracy when machining CSAM material.

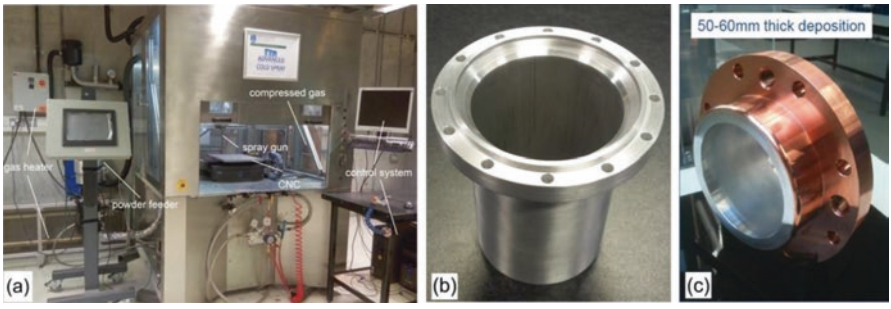

Fig. 6.2 Digital photos of (**a**) CSAM system [TCD], (**b**) CSAM aluminum flange [TCD and Moog Dublin www.moog.com], and (**c**) CSAM copper flange on aluminum tube (Abreeza et al. 2011)

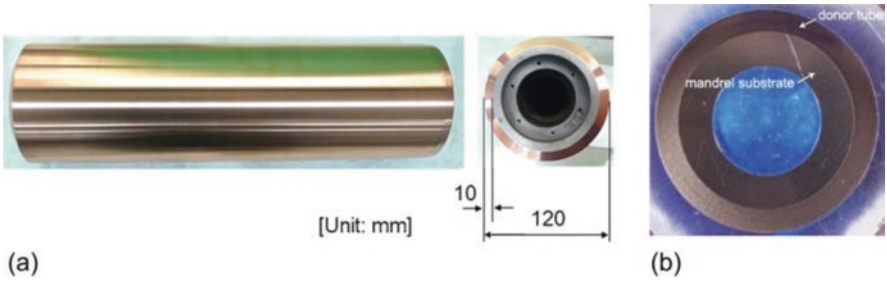

Fig. 6.3 Digital photos of CSAM rotational structure: (**a**) scaled canister for disposal of CANDU spent fuels and (**b**) tantalum-10 tungsten alloy donor tube used for the gun barrel liners (Barnett et al. 2015; Choi et al. 2010)

Subsequent property tests on this flange demonstrated that its quality completely meets the company's requirement. Similar copper flange structure coated on an aluminum tube is also provided in Fig. 6.2c (Abreeza et al. 2011).

Metal cylinder outer and inner walls can also be produced using CSAM. The fabrication process is similar to the flange fabrication, particularly for the additive manufacture or repair of external features. Figure 6.3a provides an example showing a 1/10-scaled canister for disposal of CANDU spent fuels fabricated via CSAM (Choi et al. 2010). A 10 mm thick coating layer with a porosity of 0.3%, density of 8900 kg/m^3, and oxygen content of 0.019% (that of original copper powder was 0.02%) was deposited onto the cast iron cylinder, showing great tensile strength, mechanical stability, and thermal properties. Moreover, in some circumstance, the mandrel substrate may be not needed and have to be removed after the fabrication of rotational structure. An instance is provided in Fig. 6.3b showing a CSAM tantalum-10 tungsten alloy donor tube used for the manufacture of gun barrel liners (Barnett et al. 2015). In this case, the tantalum-10 tungsten alloy layer was deposited onto a cylindrical aluminum mandrel substrate, and then the inner mandrel was removed using deep drilling, honing techniques, and a brief soak in dilute sodium hydroxide. Analogously, single material cylinder walls can be easily fabricated via CSAM with the similar procedure. More rotational outer wall components fabricated via CSAM are shown in Fig. 6.4 (Chad 2014; Kumar and Chavan 2011; May et al. 2013; Richter 2014; Sova et al. 2013).

For the manufacture of internal features, the procedure varies according to the inner diameter. If the inner diameter is sufficiently large to allow for a conventional cold spray nozzle and its holding accessories to fit inside the component, the fabrication process is same as producing the external features. If the internal diameter is too small to allow this, the nozzle can be slightly inclined to fit the limited space at the expense of lower coating quality caused by the spray angle. An example is provided in Fig. 6.5a, b, which shows a copper inner wall of a pressure ring used for food processing machine fabricated via CSAM (May et al. 2013). As can be seen, the nozzle is inclined to the target substrate during the fabrication due to the limitation of the internal diameter. Apart from the aforementioned cases, special-

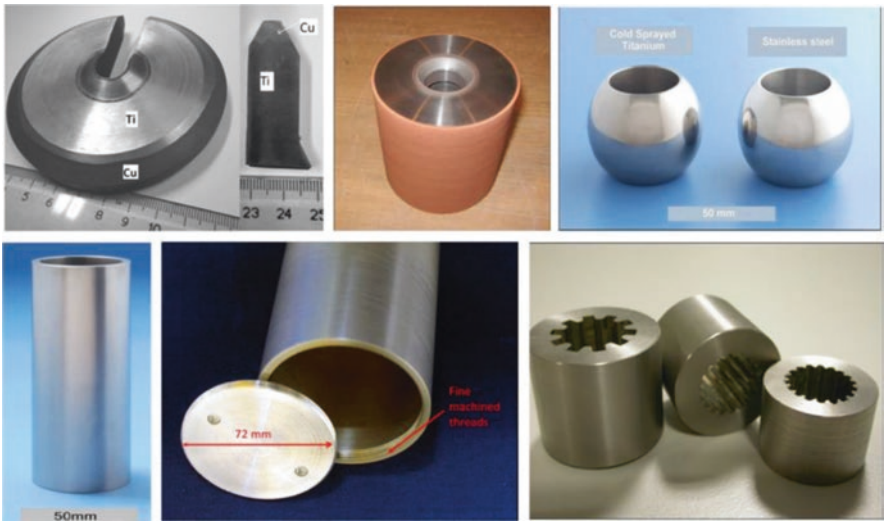

Fig. 6.4 CSAM rotational structures (Chad 2014; Kumar and Chavan 2011; May et al. 2013; Richter 2014; Sova et al. 2013)

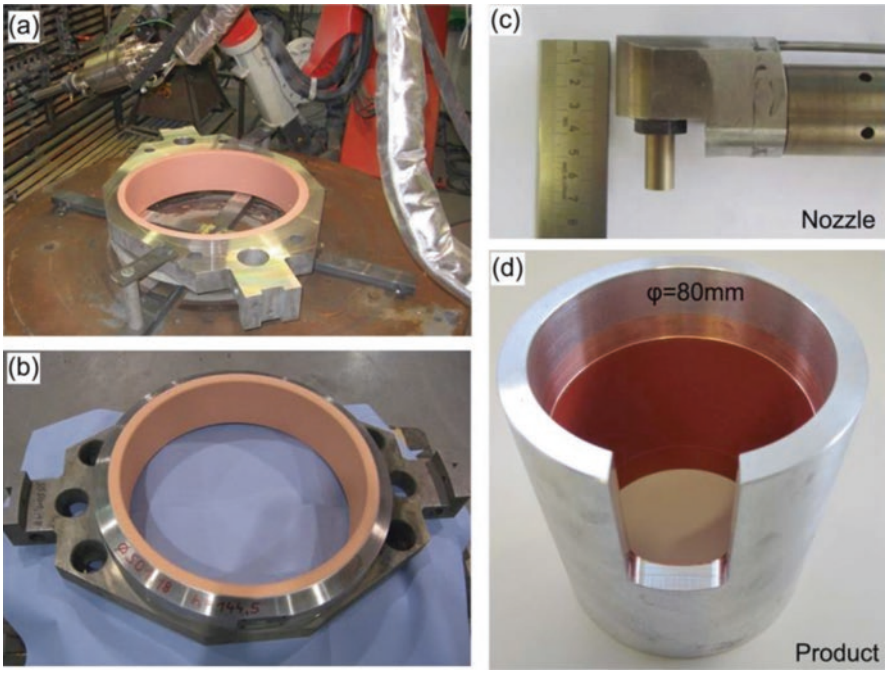

Fig. 6.5 Digital photos of CSAM rotational structures: (**a**, **b**) an inner wall of a pressure ring for food processing machine, (**c**) a micro-size cold spray nozzle, and (**d**) an inner wall of small-space cylinder tube (May et al. 2013; Richter 2014)

Fig. 6.6 Digital photos of CSAM components with complex structure: (**a**) cone structure, (**b**) gear, and (**c**) bracket (Briefing 2013; Champagne and Helfritch 2016; Richter 2014)

designed cold spray nozzles must be used if the inner diameter is very small. As illustrated in Fig. 6.5c, a micro-size cold spray nozzle (5–10 mm in length) is used for the spraying of internal features. The minimum diameter allowed to be fabricated is determined according to the coating thickness and nozzle size. Figure 6.5d shows a copper inner wall on a metal tube with the diameter of 80 mm fabricated using the micro nozzle shown in Fig. 6.5c (Richter 2014).

More complex components may be manufactured using CSAM by accurately defining the nozzle trajectory or designing a mandrel substrate. Figure 6.6 shows some complex structures fabricated via CSAM (Briefing 2013; Champagne and Helfritch 2016; Richter 2014).

The cone structure shown in Fig. 6.6a and gear shown in Fig. 6.6b were made by coordinating the nozzle motion with the rotational movement of the substrate. The bracket structure shown in Fig. 6.6c was fabricated by depositing the additive materials onto a specially designed substrate mold followed by separation of the component from the mold. The use of CSAM to fabricate complex-shape components is

promising, but relevant investigations are very limited. It is necessary to conduct more works in this field including advanced nozzle trajectory and substrate mold development.

6.2.2 *Near Net-shape Structure Fabrication*

CSAM is also capable of producing net-shape or near net-shape components. As shown in Fig. 6.7a, the fabrication process may require the use of a mask or shield to prevent the deposition of redundant materials and hence to obtain a specific pattern that is required. An example of CSAM net-shape structure is the pyramidal fin arrays used for the compact heat exchanger as shown in Fig. 6.7b (Cormier et al. 2016, 2015, 2014a, b, 2013; Dupuis et al. 2016a, b; Farjam et al. 2015). By adjusting the standoff distance and design scheme of the wire mask, the fin array shape and density can be accurately controlled (Cormier et al. 2014a, b, 2013; Farjam et al. 2015). The thermal and mechanical tests suggest that the CSAM fin arrays have superior thermal performance than traditional straight (rectangular) fins due to the higher convective heat transfer coefficient caused by increased turbulence wake behind the fins, and the roughness and porosity of the cold spray surface (Cormier et al. 2013; Farjam et al. 2015; Kotoban et al. 2016). Further studies also suggested that thermal conductance can be improved by increasing the fin height, increasing fin density, or using staggered configurations at the expense of more pressure loss (Cormier et al. 2014a; Dupuis et al. 2016b). In addition, mask-assisted CSAM also can be used to fabricate chip heat sinks, metal markings, or other products with special patterns (Bierk et al. 2011; Birtch 2010; Kashirin et al. 2011).

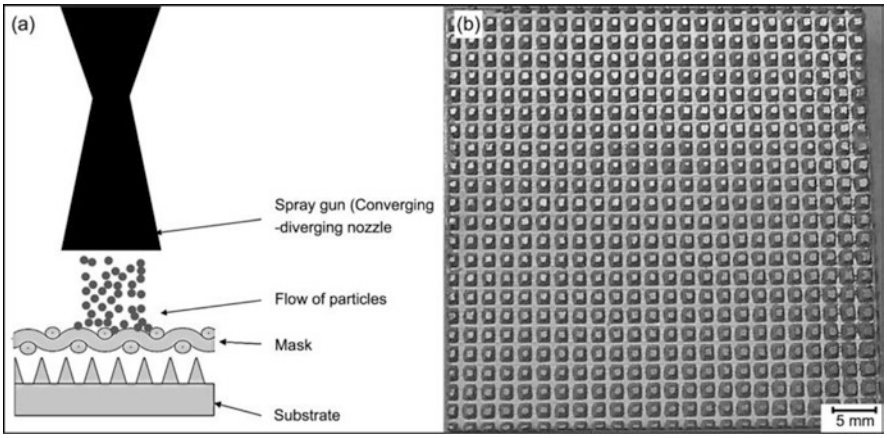

Fig. 6.7 CSAM pyramidal fin arrays heat sink. (**a**) Schematic of the fabrication process and (**b**) digital photo of the CSAM fin array heat sink (Cormier et al. 2014a)

6.3 Cold Spray Restoration Applications

6.3.1 Aircraft Component Restoration

Among all the potential application areas of CSR, the aerospace industry is the largest one because severe corrosion and wear problems always happen in aircraft components due to the harsh operating conditions experienced in service. Magnesium and magnesium alloys possess many merits (e.g., high stiffness, low density, high thermal conductivity, and excellent machinability) over other metals and thus have been widely used for fabricating aircraft transmission gearbox. However, as an electrochemically active material, magnesium and its alloys tend to corrode due to an anode reaction with other metallic materials. Thereby, magnesium gearbox housings frequently suffers from electrochemical corrosion after longtime service. Such corrosion significantly reduces the component lifetime, increasing the maintenance cost and potential failure risk. It is of great importance to properly repair the corroded zone and bring the restored component back to service. By utilizing CSR, the corroded part of the transmission gearbox can be repaired with aluminum or aluminum alloy materials. Figure 6.8 shows some CSR works on the damaged sections of transmission gearboxes (Howe 2014; Kilchenstein 2014; Schell 2016). Mechanical and corrosion tests on the repaired sections confirmed that the backfilling aluminum and aluminum alloy coatings had excellent adhesive strength, wear resistance, and corrosion resistance capability. These restored components are suitable to be

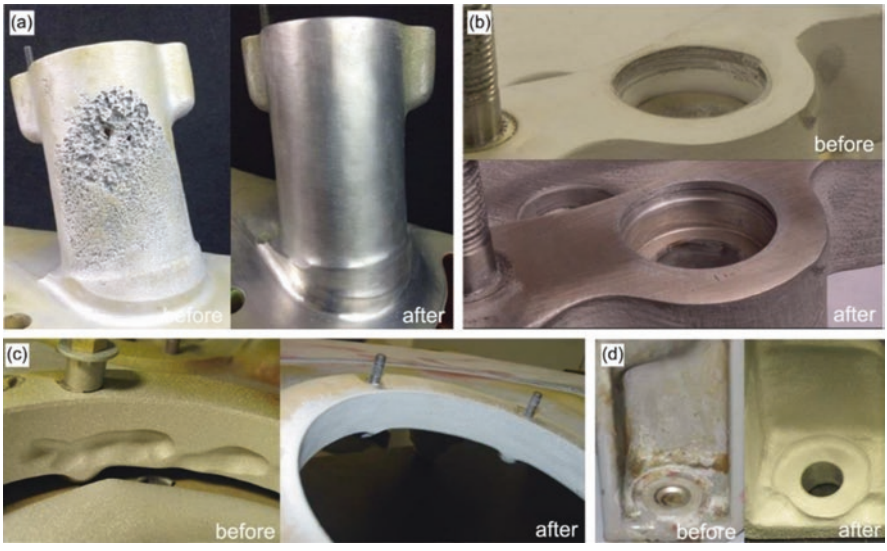

Fig. 6.8 Comparison between damaged and CSR components: (**a**) S-92 helicopter gearbox sump, (**b**) oil tube bores in CH47 helicopter accessory cover, (**c**) UH-60 helicopter gearbox sump, and (**d**) UH-60 rotor transmission housing (Howe 2014; Kilchenstein 2014; Schell 2016)

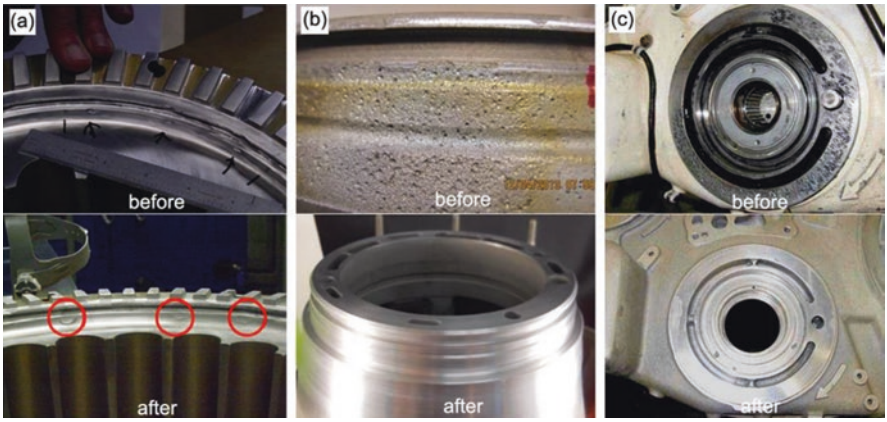

Fig. 6.9 Comparison between damaged and CSR components: (**a**) AH-64 helicopter mast support, (**b**) F18-AMAD gearbox, and (**c**) front frame of T-700 engine (Howe 2015; Kilchenstein 2014; Leyman and Champagne 2009)

returned to service after repair (Champagne et al. 2008; DeForce et al. 2007; Security and Program 2011).

Aluminum and aluminum alloy are also widely used for manufacturing aircraft components due to their low density, high tensile strength, good formability, and excellent corrosion resistance. An example of an aerospace component manufactured from aluminium alloys is the mast support on helicopters. During routine service a helicopter mast support often experiences corrosion pitting on the snap ring groove surface. When the level of the pitting damage exceeds a criterion, the mast support must be repaired or replaced. Significant savings in time and money can be achieved by repairing these components using CSR. Figure 6.9a shows a comparison between a damaged and CSR snap ring groove surface of a mast support (Leyman and Champagne 2009). The detailed restoration procedure consists of blending out corrosion pits, then filling back the removed part using aluminum-based coatings, and finally post-machining the as-coated component. Other examples of repairs using CSR are shown in Fig. 6.9 (Howe 2015; Kilchenstein 2014).

Nickel based superalloys such as Inconel are another important materials frequently used in aerospace industry due to excellent mechanical properties and high chemical and thermal resistance. Aerospace components which are likely to experience high mechanical and/or thermal loading in service are typically manufactured using nickel-based superalloys. These extreme in-service conditions often lead to severe wear and corrosion, and thus a reduction in service life for these components. An example of this is the nose wheel steering actuator barrel, which operates under high loads in a moist, dirty environment. This operating environment causes corrosion in joints. By using CSR, a corroded B737 nose wheel steering actuator barrel was repaired with nickel alloy coating. Figure 6.10 shows the comparison between a damaged and CSR B737 nose wheel steering actuator barrel. The corroded surface became smooth after repair without any pits or cracks (Schell 2016).

Fig. 6.10 Restored B737 nose wheel steering actuator barrel via CSR (Schell 2016)

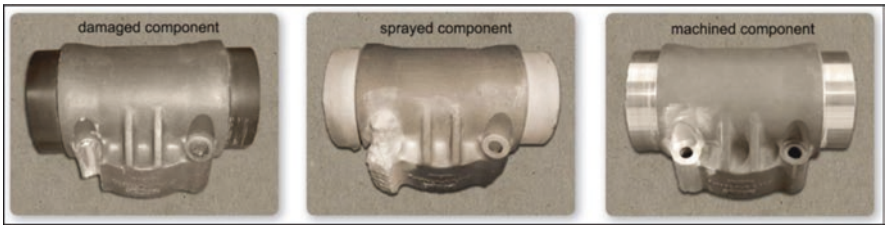

Fig. 6.11 CSR process of a mechanically damaged flap transmission tee box housing of an aircraft (Schell 2016)

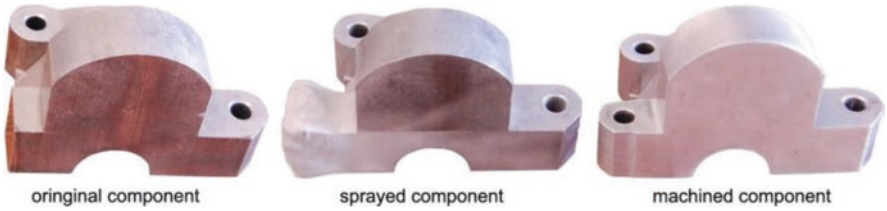

Fig. 6.12 Modification process of adding a new part onto a bearing cap via CSR (Villafuerte 2015)

CSR is also suitable for the repair of components damaged by mechanisms other than corrosion, such as fatigue, wear, or accidental overloading. Figure 6.11 shows the CSR process of a mechanically damaged flap transmission tee box housing of an aircraft (Schell 2016). It is clearly seen that the damaged component was restored to a serviceable condition after repair. Figure 6.12 shows an example of using CSR technology to add a feature to an existing component. As can be seen, a completely new component was obtained after CSR. Visually, there was no obvious boundary between the new part and original body. The new component passed the customer's quality and performance specifications (Villafuerte 2015), demonstrating the feasibility of CSR.

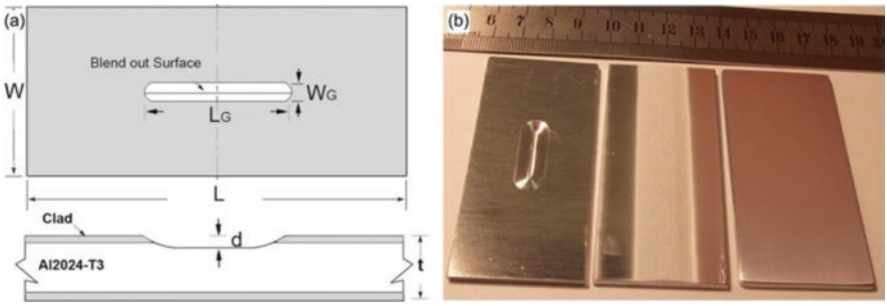

Fig. 6.13 Repair result of aluminum cladding layer on the aluminum alloy panel with self-machined damage via CSR. (**a**) Schematic of the self-machined damage and (**b**) restoration process (Yandouzi et al. 2014)

6.3.2 Aircraft Skin Restoration

Commercial and military aircraft skin are mostly made from sheets of aluminium alloy with an additional aluminum cladding layer to prevent corrosion. During routine flight, the aircraft skin is likely to suffer from erosion and scratch damages due to the high-velocity impact of dust and debris. The damaged area will allow for corrosion to penetrate through the protective aluminum clad layer and down to the base aluminum alloy. Once the base aluminum alloy is seriously corroded, fatigue properties of the component will be compromised. Therefore, it is necessary to repair the damaged aluminum cladding before the corrosion penetrates into the underlying base material. Some thermal spray technologies have been used to repair the damaged aircraft skin. However, the thermal spray coatings suffer from high porosity, high oxidation, and undesirable microstructure due to phase changes. Most importantly, the high-temperature feedstock upon impact may have an adverse effect on the properties of the underlying base material, significantly degrading the aircraft skin performance (D6–51343 2006). CSAM has great potential to resolve this problem (Jones et al. 2014, 2011; Matthews et al. 2014). Figure 6.13 shows the repair result of aluminum cladding layer on the aluminum alloy panel with self-machined damage via CSR (Yandouzi et al. 2014). Visually, the damaged area is completely filled by the cold spray aluminum coating without obvious distinction with the surrounding aluminum cladding. Mechanical tests on the repaired sample suggested that the coating hardness was higher than the original aluminum cladding and the fatigue resistance of the repaired sample was improved. In addition, corrosion testing revealed that the aluminum coating on damaged aluminum cladding provided an effective barrier to corrosion, despite the potential for corrosion to occur at the edge of the repair deposit. The testing results on the self-damaged aircraft skin coupon positively demonstrated the feasibility of CSR for the repair of aircraft skin.

In addition to the skin damage, aircraft fuselage also suffers from multisite damage (MSD) problem. For nearly all kinds of aircraft, the fuselage is fabricated through lap joints of aluminum alloy skin panels. These lap joints may be damaged

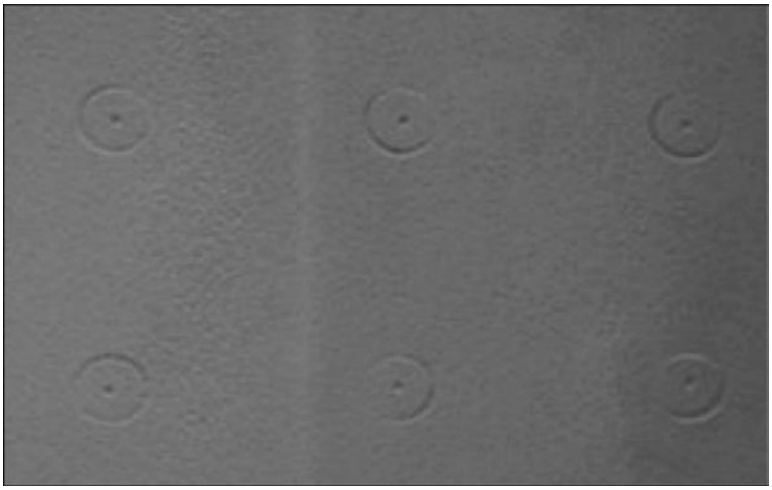

Fig. 6.14 Cold spray coating over the simulated fuselage fasteners (Matthews et al. 2014)

through accidental collisions, or through overloading in service. On one hand, fastener bore corrosion always takes place through the interface between fastener and skin despite the edge sealing between mating panels. On the other hand, multiple fastened strip repairs also act as a weak point, preferentially inducing the generation of cracks. These potential risks work together, finally causing the MSD on the aircraft skin. By using CSR combined with standard sealant, the invasion of the moisture into the joint from the interface between mating panels and also between fasteners and aircraft skin can be prevented (Jones et al. 2014, 2012; Matthews et al. 2014). Figure 6.14 shows a cold spray coating over simulated fuselage fasteners. It can be seen that the surface of the fasteners was completely sealed by the cold spray coating. Subsequent fatigue testing results indicated that the cold spray coating remained intact even when the underlying fuselage joint skin experienced MSD, positively demonstrating the capability of CSR to alleviate the corrosion damage of aircraft skin. Furthermore, CSR presented great potentials to repair the cracks caused by MSD, which helps to enhance the fuselage structural integrity (Jones et al. 2014, 2011; Matthews et al. 2014).

6.3.3 Aircraft Blade Restoration

The restoration of aluminum alloy aircraft blades is another important application of CSR. Similar to the aircraft skin, aircraft blades also suffer from serious erosion due to the high-velocity impact by dust, debris, and water droplets during service. Moreover, relatively large debris raised during aircraft taking off and landing will

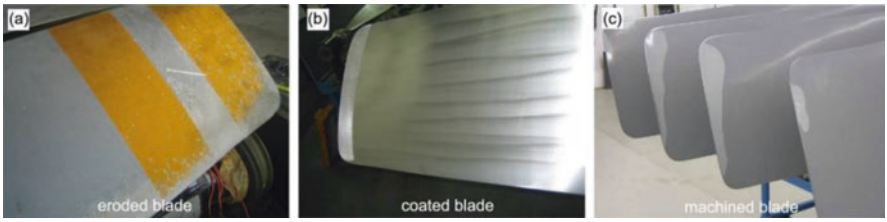

Fig. 6.15 CSR process of aluminum alloy blades (Stoltenhoff and Zimmermann 2012)

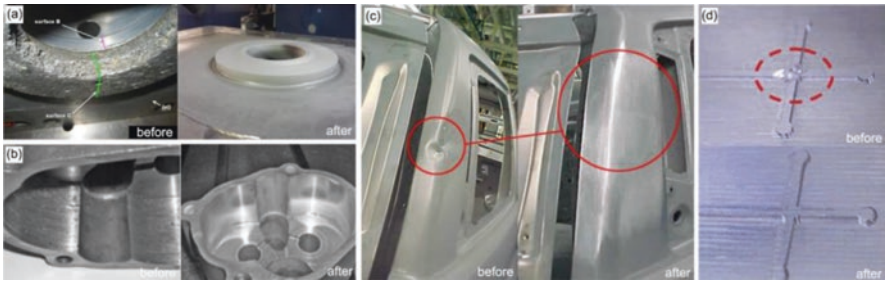

Fig. 6.16 Comparison between damaged and CSR components: (**a**) an internal bore surface of a navy valve actuator, (**b**) an oil pump housing of Caterpillar engine, (**c**) a large cast automotive part, and (**d**) a mold (Lee et al. 2007; Lyalyakin et al. 2016; Maev et al. 2014; Widener et al. 2016)

lead to more serious damage to the blade surface. The current method to repair this damage is to grind the eroded blade to a level that the damaged area has been removed. By using CSR, the lost materials during the grinding process can be filled, which allows the restoration of the original blade dimensions. Figure 6.15 illustrates the repair process of aluminum alloy blades via CSR. The restored blades have passed an extensive airworthiness test program and have been returned to service (Stoltenhoff and Zimmermann 2012).

6.3.4 Other Component Restoration

Some practical CSR works in various industries, e.g., automotive, marine, and energy, are introduced in this section. In terms of marine industry, CSR has been successfully applied to repair a corroded internal bore surface of a navy aluminum alloy valve actuator without thermally affecting the base material, showing superior capability over other traditional repair method (i.e., tungsten inert gas welding, metal inert gas welding, and laser cladding). Figure 6.16a shows the comparison between the damaged and CSR actuator. The CSR actuator has passed all property

tests and is now back in service (Widener et al. 2016). In the automotive industry, CSR has been applied to repair the corroded oil pump housing of Caterpillar-3116 and Caterpillar-3126 engines (Fig. 6.16b). It was reported that more than 30 such corroded pump housings were restored via CSR from 2012 to 2013 in Moscow. All of these reconditioned components have been returned to service without any failure reports so far (Lyalyakin et al. 2016). Moreover, CSR was also used to repair severe cracks in large cast automotive parts as can be seen in Fig. 6.16c (Maev et al. 2014). Additionally, restoration of damaged molds is also possible using CSR as shown in Fig. 6.16d. The repaired mold presented similar results during the cutting force test and even better wear resistance capability than original one (Lee et al. 2007). These are only some of the potential applications for CSR, which is still a developing technique.

6.4 Processing Parameters During Manufacturing

6.4.1 Introduction of Processing Parameters

Processing parameters including nozzle moving speed, spray distance, spray angle, scanning step, and nozzle trajectory play an important role in CSAM and CSR. These parameters are known to pose direct impact on the particle impact velocity and landing footprint; thereby they may affect the consequent coating thickness, coating deposition efficiency, coating cross-sectional profile, and coating properties. Understanding the effects of these parameters is necessary to achieve the desired deposition geometry. Figure 6.17 shows schematic of the processing parameters in CSAM and CSR.

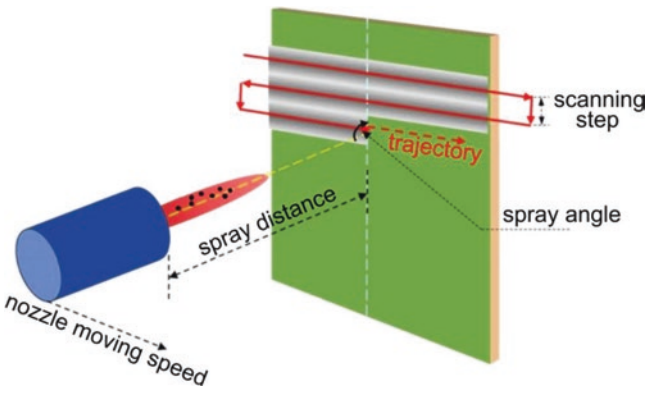

Fig. 6.17 Schematic of the processing parameters in CSAM and CSR

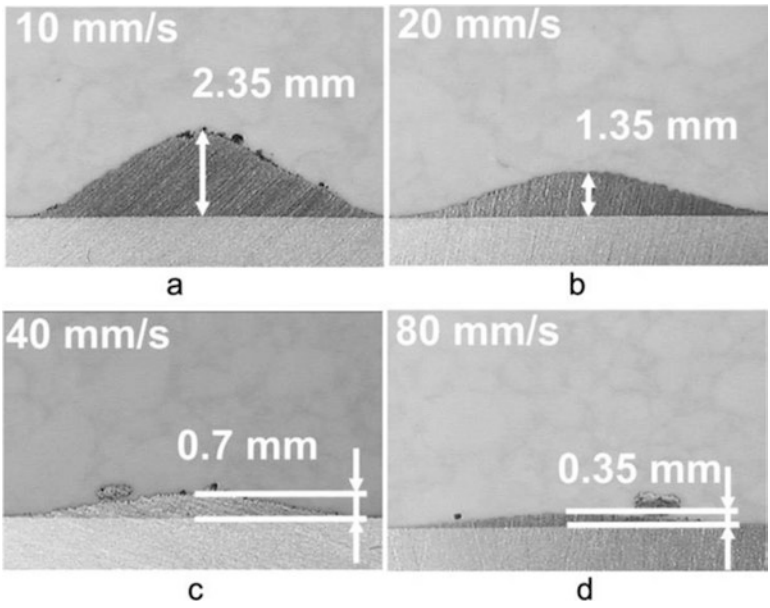

Fig. 6.18 Effect of nozzle moving speed on the single-track coating thickness and cross-sectional profile (Kotoban et al. 2016)

6.4.2 Nozzle Moving Speed

Nozzle moving speed is a parameter that determines the spray duration and amount of feedstock powder impacting onto the target surface. The direct effect of nozzle moving speed is on the coating thickness. Higher nozzle moving speed results in lower single-track coating thickness as shown in Fig. 6.18 (Deng et al. 2014; Fang et al. 2010; Kotoban et al. 2016; Yin et al. 2015). An extreme case is the single particle deposition where the nozzle speed is so high that individual splats are not in contact with each other (Yin et al. 2015). It was reported that increasing coating thickness leads to the increment of residual stress and bonding strength (Moridi et al. 2014; Rech et al. 2014; Xiong et al. 2015); thereby nozzle moving speed also poses indirect impact on these mechanical properties. Moreover, nozzle moving speed was found to influence the single-track coating cross-sectional profile through affecting the deposition efficiency (C. Chen et al. 2016a, b; Kotoban et al. 2016; Pattison et al. 2007; Sova et al. 2013). As can be seen from Fig. 6.18, the cross-sectional profile becomes gradually sharper as the coating thickness increases. The substantial reason behind this phenomenon is the flow characteristic of the propulsive gas passing through a supersonic nozzle. According to fluid dynamics theory, the particle velocity and the consequent deposition efficiency at the central zone are higher than that at the outer zone (Champagne et al. 2011; Tabbara et al. 2011; Yin

et al. 2014). Thereby, the coating cross-sectional profile presents a Gaussian shape as shown in Fig. 6.18a. The slope of this profile causes deposition to occur at angles less than 90 degrees, further decreasing the deposition efficiency. This reduction in deposition efficiency, in turn, leads to preferential deposition along the peak compared to the sloped edges. Finally, the profile becomes increasingly shaper as the nozzle moving speed decreases. In addition, another potential effect of nozzle moving speed is the heating input from the high-temperature impinging jet to the coating and substrate. Low nozzle moving speed helps the temperature increment of the deposited coating and substrate. This fact may contribute to the deposition of subsequent coating (Yin et al. 2015) but in turn may result in the development of thermal stress (Candel and Gadow 2009).

6.4.3 Spray Distance

Spray distance is defined as the distance between the nozzle outlet and the target surface, significantly affecting the particle impact velocity and the consequent coating properties. In a supersonic-free jet, the intensity of the jet core decreases gradually along the jet central axis due to the momentum exchange between the jet and the atmosphere. Inside the jet core, particles achieve positive drag force and thus rapidly accelerate. However, after the jet core length is exceeded, the gas velocity becomes lower than the particle velocity, and the resultant negative drag force causes the deceleration of particles. As a result, the particle impact velocity and deposition efficiency increases with increasing spray distance up until an optimum value is reached, after which the particle velocity and deposition efficiency drop. This fact has been experimentally confirmed (Cai et al. 2014; Pattison et al. 2008). However, different results were also reported in some works, showing a monotonic reduction of coating thickness (deposition efficiency) with increasing the spray distance (Han et al. 2005; Li et al. 2008). Note that coating thickness will increase with the particle impact velocity when the coating deposition efficiency is less than 100%. The different results reported in these publications show that the role of spray distance in the particle velocity upon impact and deposition efficiency is still not quite clear. More research on this subject should be carried out in the future. Despite having different results, a common suggestion is that the spray distance should not be excessively large.

6.4.4 Spray Angle

Spray angle is defined as the angle of the nozzle axis to the target surface. It has a significant influence on the particle impact velocity components and consequent coating properties. When spraying at an angle to the substrate, only the normal velocity component contributes to the coating deposition, while the tangential

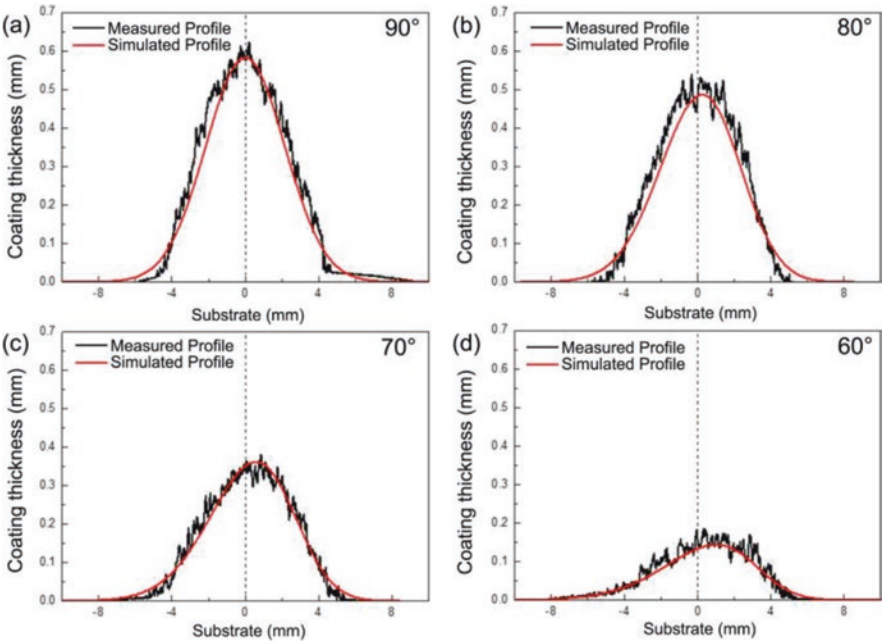

Fig. 6.19 Effect of spray angle on the single-track coating cross-sectional profile (C. Chen et al. 2016a, b)

velocity component plays an opposite role by potentially detaching the deposited particles. As the spray angle decreases, the normal velocity component reduces, while the tangential velocity component increases. As a consequence, coating deposition efficiency and thickness reduce, and the coating bonding strength and porosity decrease (Binder et al. 2011; Gilmore et al. 1999; Li et al. 2006, 2005; Luo et al. 2016; Yin et al. 2013). Therefore, the nozzle should be maintained in a normal orientation to the substrate during the coating fabrication process. Furthermore, spray angle also affects the single-track coating cross-sectional profile due to the variation in spray distance over the particles impact area. Therefore, the cross-sectional profile normally presents a skewed shape as shown in Fig. 6.19 (C. Chen et al. 2016a, b).

6.4.5 Nozzle Scanning Step

Coating buildup is achieved through nozzle scanning over the entire target surface line by line according to a predefined trajectory. The coating is formed by the partial overlapping of many single-track coatings. Scanning step is defined as the interval between two single-track coatings, which is an important parameter that determines the stack process. The main influence of scanning step is the coating thickness

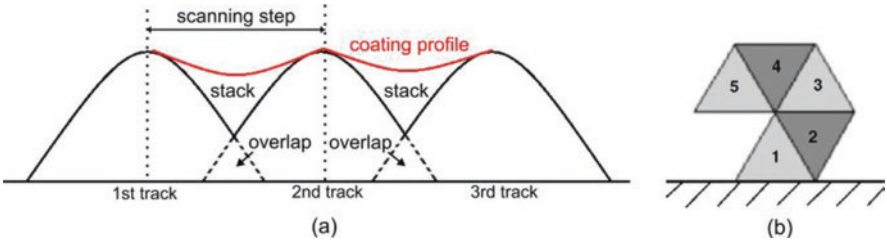

Fig. 6.20 Schematic of scanning strategy (Cai et al. 2014; Pattison et al. 2007)

uniformity and surface morphology. Two scanning strategies are commonly used to achieve a uniform coating thickness. The first approach is to use a scanning step less than half of the width of a single deposited line. When the scanning step is small, the neighboring tracks can overlap each other (Cai et al. 2014). Such overlapping compensates the thickness difference between the central peak and the slope zone of each track as shown in Fig. 6.20a, contributing to the uniformity of coating thickness. The other strategy is to use a larger scanning step, and offset subsequent deposited layers to create a uniform coating thickness. In this way, the neighboring tracks at the first layer do not overlap each other, while the track at the second layer is deposited on the gap between two first-layer tracks as illustrated in Fig. 6.20b (Pattison et al. 2007). In this case, the gap can be perfectly filled, and a smooth coating surface also can be achieved. Investigations on the scanning strategy are still quite limited; more work should be carried out to compare existing strategies, develop new strategy, and explore their influence on the coating properties.

6.4.6 Trajectory Definition

The basic principle of trajectory definition is to maximise the coating homogeneity and quality. The as-sprayed coating should possess a homogenous density, property, and bonding strength. To achieve this objective, the processing parameters must be carefully chosen before spraying and kept constant during the coating fabrication process. When spraying on a flat surface, a simple round-trip trajectory is mostly applied to maximise coating homogeneity. However, for a complex curved surface which could be experienced in CSAM and CSR applications, trajectory definition should maintain the constant spray distance, spray angle, nozzle speed, and other processing parameters over the target surface to avoid the inhomogeneity of coating. Therefore, more advanced nozzle trajectory planning is required. To date, very few attempts have been made for the development of such advanced trajectory in CSR and CSAM (Cai et al. 2016; Chaoyue Chen et al. 2016a, b). A recent study by Chen et al. reported a novel spiral trajectory for a CSR self-damaged aluminum coupon. Figure 6.21 shows the spiral trajectory and the CSR coupon before final machining. The results indicated that spiral trajectory improved the surface

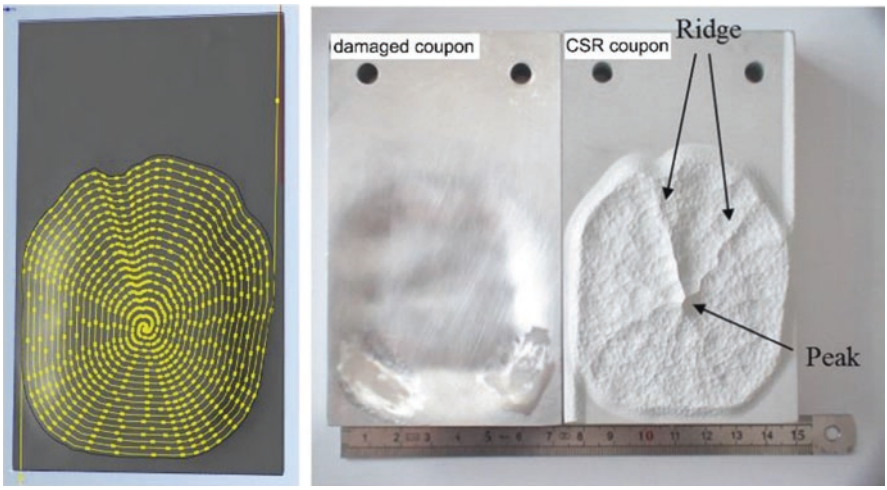

Fig. 6.21 Spiral trajectory and the CSR coupon before final machining (Chaoyue Chen et al. 2016a, b)

condition of as-repaired coupon and reduced deposition of redundant material compared with round-trip trajectory (Chaoyue Chen et al. 2016a, b). This fact indicates that nozzle trajectory is an important parameter for CSR and thus warrants further investigation.

6.5 Robotic Control of Processing Parameters

6.5.1 Introduction of Robotic Control

The precise control of nozzle motion is essential to the fabrication of high-quality CSAM and CSR products. To achieve this, industrial robots (including multi-axes robot arm and computer numerical control platform) are frequently used in cold spray process to control the nozzle or substrate. By properly programming the robot, processing parameters including nozzle moving speed, spray distance, spray angle, and scanning step, as well as nozzle moving trajectory can be accurately planned and executed. Programming also allows for multiple repetitive spraying cycles to be carried out with ease. In addition, the remote control system of a robot allows human operators to work far away from the high-temperature, high-noise, and high-dust environment. Due to these advantages, industrial robots are widely applied to assist the cold spray process for coating fabrication, CSAM, and CSR.

In general, before starting CSAM or CSR work, a spray strategy must be decided upon, and the robot must be programmed to define the processing parameters and nozzle moving trajectory. Then, the compiled program will be uploaded to and

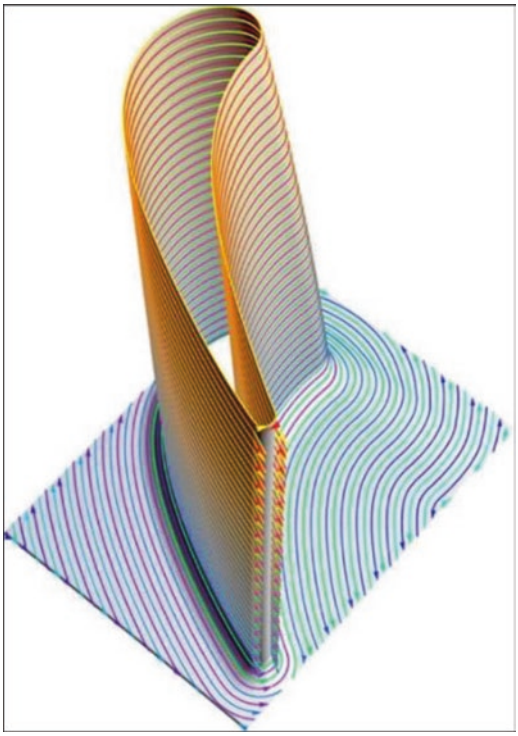

Fig. 6.22 Trajectory on the turbine blade defined by off-line programming method (Stier 2014)

implemented by the robot. According to the complexity of the task, a program can be written in various ways. For a simple task such as when the substrate is a flat surface with a regular shape, the online programming method is always applied, where the processing parameters and trajectory are created through manually defined motion instructions and target points. However, for surfaces with complex topography, e.g., the turbine blade surface shown in Fig. 6.22, the processing parameters and trajectory should be carefully created according to the working strategy, and the off-line programming platform by the aid of CAD/CAM software is more suitable (Cai et al. 2016, 2015; Chaoyue Chen et al. 2016a, b; Deng et al. 2012; Stier 2014). In addition, the trajectory definition must consider the inertia and kinematics of the robot arm to optimize the nozzle moving speed (Deng et al. 2014; Fang et al. 2010).

6.5.2 Online Programming

The online programming method has been widely used to assist cold spray work (Deng and Chen 2015). In this method, the processing parameters and spray trajectory are created by manually defining the motion instructions and target points. The

robot motion instructions which contains the data for motion type, target point details, nozzle traverse speed, and reference coordinate system is firstly created. The nozzle is then moved to the first target point to record its position and orientation information and then moved to the next point. By repeating this procedure until the last target point, all target point locations can be recorded, and the nozzle moving trajectory is finally created. The robot will follow this predefined motion instructions and nozzle moving trajectory to finish the task. The online programming is relatively easy to learn and apply. It is suitable for the simple tasks where trajectory is on a planar surface and only a small quantity of target points need to be defined. However, as most of the programming work is finished on the control panel, the online programming method lacks accuracy and efficiency when the target points are in a large number or on a curved surface. Therefore, as stated previously, this method is only recommended for implementing simple tasks.

6.5.3 Off-Line Programming

Off-line programming is a more advanced and accurate method for trajectory definition compared with online programming (Deng and Chen 2015). It is applicable for tasks where the workpieces have complex geometries and high precision requirement (see Figs. 6.21 and 6.22).

The rapid development of CSAM and CSR brings increasing demands of off-line programming to precisely define the trajectory of the nozzle. For this method, the trajectory can be defined by the aid of graphic operation interface and trajectory generation algorithm. Firstly, the geometry of the workpiece is obtained through either CAD/CAM software or by measurement of the surface geometry depending on the complexity of the task. Afterward, the acquired 3D geometry is input into a simulator platform for trajectory generation and robot moving simulation. In the simulator platform, the trajectory and robot motion data can be easily accessed and adjusted. Finally, these data are converted to the programming language and uploaded to the robot for execution. The detailed flowchart of the off-line programming is provided in Fig. 6.23 (Deng et al. 2012). The off-line programming and robotics simulator tools help robot integrators to create the optimal trajectory for the robot to perform a specific task. For this method, the robot program is created in an external computer and then uploaded to the robot for execution; thus it does not delay the production process.

In order to provide a more intuitive introduction to the off-line programming, the commercial software named RobotStudio™ which designed for use with ABB robots (ABB Automation Technology Products AB, Gothenburg, Sweden) is selected as an example. Figure 6.24 shows the screenshot of working interface in RobotStudio™. As can be seen, the robot and workpieces are represented by 3D geometries in the software to simulate the real working environment. Then, the trajectory generated on the target surface is simulated by the virtual robot system available in RobotStudio™. By analyzing simulation results (i.e., the

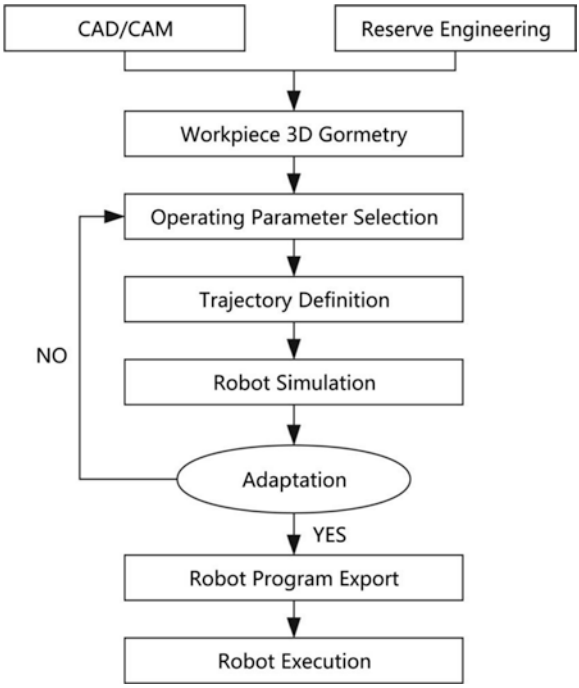

Fig. 6.23 Flowchart of the off-line programming method (Deng et al. 2012)

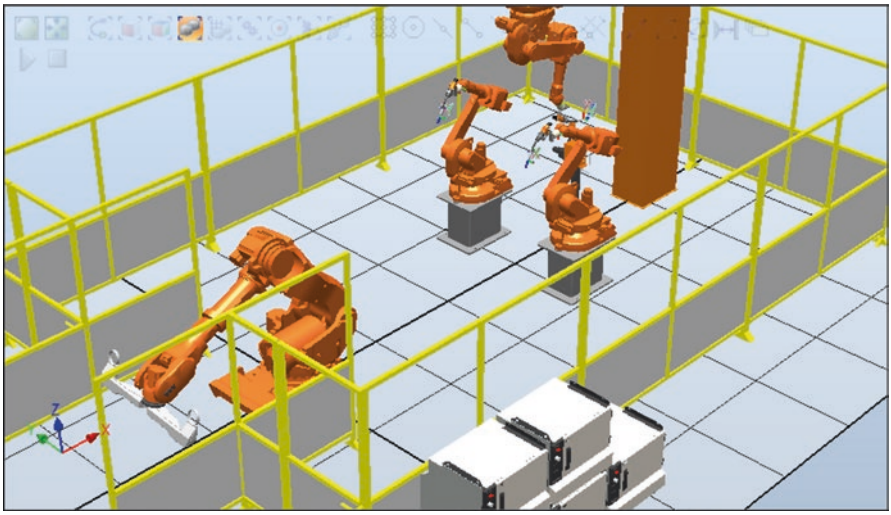

Fig. 6.24 Screenshot of working interface in RobotStudio™ (Deng and Chen 2015)

nozzle speed and the joint position of each axis), the processing parameters and trajectory are optimized. Finally, the optimal trajectory is uploaded to the robot for execution.

6.5.4 External Axis

The mandrel substrate surface often has rotational symmetry in CSAM, but the robot arm is difficult to move in a circular trajectory around the target surface due to its limited reachability. In this regard, an external axis for holding the workpieces is normally required to assist the manufacturing process. Specifically, the robot trajectory can be simplified into a linear motion that cooperates with the rotation of the workpiece by external axis. The coating thickness can be adjusted by controlling the linear movement speed of robot and rotation speed of external axis. For more complicated CSAM tasks, e.g., hook gear and turbo blade, the robot and external axis must be linked through software in order to generate the specific trajectory for fabrication.

6.6 Post-Machining and Finishing Processes

6.6.1 Post-Machining Process

Cold spray typically leaves a rough, undulating, porous surface after spraying. In many applications, such as in repair of a worn surface using cold spray, the as-sprayed surface is not suitable for immediate use, either due to surface finish, wear behavior (Lee et al. 2007), or dimensional accuracy requirements. This necessitates the use of a machining or finishing process. To date, relatively little research has been undertaken into the machinability of cold spray materials.

Cold spray deposits are generally suitable for normal machining processes, such as turning, milling, or drilling (Sova et al. 2013) (Barnett et al. 2015). However, due to the unique properties of cold spray material, careful selection of machining parameters is required to achieve a satisfactory finish. An example of a CSAM component being machined into a finished part is shown in Fig. 6.2b, where turning and drilling operations have been used to manufacture a flange.

In order to understand the machining of cold spray materials, it is important to recognize that unless the coating has been brought to full density, through hot isostatic pressing (HIP) or a similar method, it will machine in a similar manner to a porous, cast material. As a cold spray coating is an amalgamation of individual particles, there will be variations in density and levels of work hardening within the coating, with the potential for small oxide inclusions (Yin et al. 2012). This will cause variations in the physical and thermal loads experienced by any cutting tools.

Many comparisons can be made between the machining of cold spray materials and materials produced through powder metallurgy (Czampa et al. 2013) and electron beam melting (Aziz et al. 2012; Bordin et al. 2014; Montevecchi et al. 2016), which are acknowledged as more difficult to machine than bulk materials. If a deposit has poor inter-particle bonding and little particle deformation, then the cutting process will resemble that of a sintered material, with inter-particle bonds being broken and no chips being formed. The surface finish after machining of any such material would be porous and undulating, though some smearing and densification of the surface may be observed (Tutunea-Fatan et al. 2011). Conversely, a fully dense deposit which has good ductility will form chips and machine in a very similar manner to the bulk material. Thus, the machinability of a cold spray deposit is dependent upon the density and ductility of the cold spray coating created. Cutting forces during the machining of porous cold spray coating will typically be lower than that of bulk material but with more variation during cutting. Porous materials manufactured using other techniques typically show lower but more variable cutting forces (Abolghasemi Fakhri et al. 2012), with the lower magnitude of the forces being at least partially attributable to the lower stiffness of porous materials (Lu et al. 1999) and the variation due to the discontinuous cutting action experienced as the tool disengages and then reengages when passing through pores. Cold spray coatings with higher ductility will show less variation in cutting forces, while coatings with lower porosity will show higher cutting forces. Other issues which are of interest in the machining of cold spray deposits are the potential for debonding of the cold spray coating if overly aggressive cutting parameters are used or if a large portion of the bond area is removed during machining. If it is necessary to remove the deposit from the substrate in order to achieve the geometry required, this should be done first, as the deposit may distort due to residual stresses after debonding. Careful inspection should be carried out of the component after machining, as cut-induced cracking has been observed to cause failure in tensile test samples machined from cold spray coating (MacDonald et al. 2016). Little to no research has been carried out into tool wear during the machining of cold spray materials. It can be expected that due to the discontinuous nature of the machining process, tool wear will be greater than that observed when machining bulk material. The use of tamping materials in cold spray such as alumina, which are typically very hard, will cause excessive tool wear during machining (Ramulu et al. 2002).

6.6.2 Finishing Process

Little research has been carried out into the use of grinding as a manufacturing process for cold spray coatings. However, the use of epoxy resin SiC grinding paper to prepare polished cross-section samples of cold spray samples is common in research (Goldbaum et al. 2016; Jakupi et al. 2015; Morgan et al. 2004; Villa et al. 2013). As with cutting processes, often there will be densification and smearing caused by individual grits plowing the surface rather than cutting (Tutunea-Fatan et al. 2011).

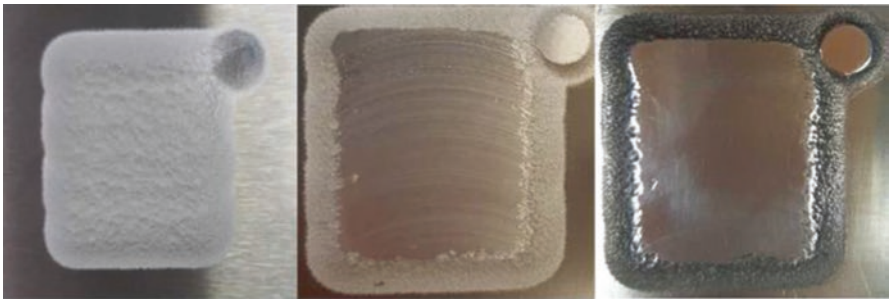

Fig. 6.25 Aluminum cold spray coating, showing as-sprayed, after face milling and after polishing

An example of a machining and finishing process which was carried out in TCD is shown in Fig. 6.25. After face milling the surface has visible machining marks, which are removed after grinding and polishing. Microscope inspection of the surface after polishing shows no visible porosity, which indicates that the material has smeared and flowed to form a fully dense surface layer.

6.7 Conclusions and Future Perspectives

Cold spray technology has shown great potential in additive manufacturing and damaged component restoration due to its great ability to retain the original feedstock properties and prevent adverse influence on the underlying substrate materials. A variety of components have been successfully fabricated or repaired via CSAM and CSR. When compared to materials manufactured using other additive manufacturing techniques, CSAM products were found to possess sufficiently high quality, while CSR components mostly had equal or even better performance in comparison with the original (undamaged) ones. Despite having significant achievements, CSAM and CSR still have a lot of aspects to be explored or improved. CSAM for fabrication of complex components will still be an interesting and challenging subject. Currently, most of the existing CSAM works concern about simple rotational structures, while relatively little work has been done on the manufacture of complex structures, e.g., cone, gear, and bracket. In order to broaden the product variety of CSAM, more works should be done in the coordination of nozzle motion and external axis rotation, mandrel substrate design, and the post-spraying machining of the deposited material. Micro-nozzle development is also encouraged as this is of great importance to the deposition of internal features within existing components. As for the CSR, it is necessary to establish standard testing procedures for restored components and also to explore potential application fields. Nozzle motion parameters, scanning strategy, and trajectory optimization should be another focal point of the future work. This will help to reduce the material's waste and the post-machining work caused by the imprecise

over-deposition on the damaged area. Also, an effective solution of poor deposition on the small-angle corner should be further investigated as it is now a limitation for CSR to broaden its applications.

References

Abolghasemi Fakhri M, Bordatchev EV, Tutunea-Fatan OR (2012) An image-based methodology to establish correlations between porosity and cutting force in micromilling of porous titanium foams. Int J Adv Manuf Technol 60:841–851. https://doi.org/10.1007/s00170-011-3647-1

Abreeza M, Yuji I, Kazuhiro O (2011) Computational simulation for cold sprayed deposition. ELyT Laboratory Workshop, Sendai

Aziz MSA, Ueda T, Furumoto T, Abe S, Hosokawa A, Yassin A (2012) Study on machinability of laser sintered materials fabricated by layered manufacturing system: influence of different hardness of sintered materials. Procedia CIRP 4:79–83. https://doi.org/10.1016/j.procir.2012.10.015

Barnett B, Trexler M, Champagne V (2015) Cold sprayed refractory metals for chrome reduction in gun barrel liners. Int J Refract Met Hard Mater 53:139–143. https://doi.org/10.1016/j.ijrmhm.2015.07.007

Bierk B, Mgr G, Addison G, Elmquist B (2011) Repair Technology Development Projects, In: CSAT Workshop. Worcester, USA

Binder K, Gottschalk J, Kollenda M, Gärtner F, Klassen T (2011) Influence of impact angle and gas temperature on mechanical properties of titanium cold spray deposits. J Therm Spray Technol 20:234–242. https://doi.org/10.1007/s11666-010-9557-1

Birtch W (2010) Practical cold spray. https://www.supersonicspray.com. Accessed 3 June 2014

Blose RE, Walker BH, Walker RM, Froes SH (2006) New opportunities to use cold spray process for applying additive features to titanium alloys. Met Powder Rep 61:30–37. https://doi.org/10.1016/S0026-0657(06)70713-5

Boeing Standards D6-51343 (2006) Thermal spray repair of exterior clad aluminum. USA

Bordin A, Ghiotti A, Bruschi S, Facchini L, Bucciotti F (2014) Machinability characteristics of wrought and EBM CoCrMo alloys. Procedia CIRP 14:89–94. https://doi.org/10.1016/j.procir.2014.03.082

Briefing T (2013) Metal coated particles and defense applications. In: CSAT Workshop. Worcester, USA

Cai Z, Deng S, Liao H, Zeng C, Montavon G (2014) The effect of spray distance and scanning step on the coating thickness uniformity in cold spray process. J Therm Spray Technol 23:354–362. https://doi.org/10.1007/s11666-013-0002-0

Cai Z, Liang H, Quan S, Deng S, Zeng C, Zhang F (2015) Computer-aided robot trajectory autogeneration strategy in thermal spraying. J Therm Spray Technol 24:1235–1245. https://doi.org/10.1007/s11666-015-0282-7

Cai Z, Chen T, Zeng C, Guo X, Lian H, Zheng Y, Wei X (2016) A global approach to the optimal trajectory based on an improved ant Colony algorithm for cold spray. J Therm Spray Technol 25:1631–1637. https://doi.org/10.1007/s11666-016-0468-7

Candel A, Gadow R (2009) Trajectory generation and coupled numerical simulation for thermal spraying applications on complex geometries. J Therm Spray Technol 18:981–987. https://doi.org/10.1007/s11666-009-9338-x

Chad H (2014) CSIRO Titanium Technologies and Additive Manufacturing, Future Manufacturing Flagship. https://www.atse.org.au/Documents/Events/SA%20Manufacturing/chad-henry-titanium-technologies.pdf. Accessed 13 Nov 2016

Champagne V, Helfritch D (2016) The unique abilities of cold spray deposition. Int Mater Rev 6608:1–19. https://doi.org/10.1080/09506608.2016.1194948

Champagne VK, Helfritch D, Leyman PF (2008) Magnesium repair by cold spray. Plat Surf Finish 95:19–28

Champagne VK, Helfritch DJ, Dinavahi SPG, Leyman PF (2011) Theoretical and experimental particle velocity in cold spray. J Therm Spray Technol 20:425–431. https://doi.org/10.1007/s11666-010-9530-z

Chen C, Gojon S, Xie Y, Yin S, Verdy C, Ren Z, Liao H, Deng S (2016a) A novel spiral trajectory for damage component recovery with cold spray. Surf Coat Technol. https://doi.org/10.1016/j.surfcoat.2016.10.096

Chen C, Xie Y, Verdy C, Liao H, Deng S (2016b) Modelling of coating thickness distribution and its application in offline programming software. Surf Coat Technol. https://doi.org/10.1016/j.surfcoat.2016.10.044

Choi HJ, Lee M, Lee JY (2010) Application of a cold spray technique to the fabrication of a copper canister for the geological disposal of CANDU spent fuels. Nucl Eng Des 240:2714–2720. https://doi.org/10.1016/j.nucengdes.2010.06.038

Cormier Y, Dupuis P, Jodoin B, Corbeil A (2013) Net shape fins for compact heat exchanger produced by cold spray. J Therm Spray Technol 22:1210–1221. https://doi.org/10.1007/s11666-013-9968-x

Cormier Y, Dupuis P, Farjam A, Corbeil A, Jodoin B (2014a) Additive manufacturing of pyramidal pin fins: height and fin density effects under forced convection. Int J Heat Mass Transf 75:235–244. https://doi.org/10.1016/j.ijheatmasstransfer.2014.03.053

Cormier Y, Dupuis P, Jodoin B, Corbeil A (2014b) Mechanical properties of cold gas dynamic-sprayed near-net-shaped fin arrays. J Therm Spray Technol 24:476–488. https://doi.org/10.1007/s11666-014-0203-1

Cormier Y, Dupuis P, Jodoin B, Ghaei A (2015) Finite element analysis and failure mode characterization of pyramidal fin arrays produced by masked cold gas dynamic spray. J Therm Spray Technol 24:1549–1565. https://doi.org/10.1007/s11666-015-0317-0

Cormier Y, Dupuis P, Jodoin B, Corbeil A (2016) Pyramidal fin arrays performance using streamwise anisotropic materials by cold spray additive manufacturing. J Therm Spray Technol 25:170–182. https://doi.org/10.1007/s11666-015-0267-6

Czampa M, Markos S, Szalay T (2013) Improvement of drilling possibilities for machining powder metallurgy materials. Procedia CIRP 7:288–293. https://doi.org/10.1016/j.procir.2013.05.049

DeForce B, Eden T, Potter J, Champagne V, Leyman P, Helfritch D (2007) Application of aluminum coatings for the corrosion protection of magnesium by cold spray. In: Tri-Service Corrosion Conference. Denver, USA

Deng S, Chen C (2015) Generation of robot trajectory for thermal spray. In: Adams W (ed) Robot kinematics and motion planning. Nova Science Publishers, New York

Deng S, Cai Z, Fang D, Liao H, Montavon G (2012) Application of robot offline programming in thermal spraying. Surf Coat Technol 206:3875–3882. https://doi.org/10.1016/j.surfcoat.2012.03.038

Deng S, Liang H, Cai Z, Liao H, Montavon G (2014) Kinematic optimization of robot trajectories for thermal spray coating application. J Therm Spray Technol 23:1382–1389. https://doi.org/10.1007/s11666-014-0137-7

Dupuis P, Cormier Y, Fenech M, Corbeil A, Jodoin B (2016a) Flow structure identification and analysis in fin arrays produced by cold spray additive manufacturing. Int J Heat Mass Transf 93:301–313. https://doi.org/10.1016/j.ijheatmasstransfer.2015.10.019

Dupuis P, Cormier Y, Fenech M, Jodoin B (2016b) Heat transfer and flow structure characterization for pin fins produced by cold spray additive manufacturing. Int J Heat Mass Transf 98:650–661. https://doi.org/10.1016/j.ijheatmasstransfer.2016.03.069

Fang D, Deng S, Liao H, Coddet C (2010) The effect of robot kinematics on the coating thickness uniformity. J Therm Spray Technol 19:796–804. https://doi.org/10.1007/s11666-010-9470-7

Farjam A, Cormier Y, Dupuis P, Jodoin B, Corbeil A (2015) Influence of alumina addition to Aluminum fins for compact heat exchangers produced by cold spray additive manufacturing. J Therm Spray Technol 24:1256–1268. https://doi.org/10.1007/s11666-015-0305-4

Gilmore DL, Dykhuizen RC, Neiser RA, Roemer TJ, Smith MF (1999) Particle velocity and deposition efficiency in the cold spray process. J Therm Spray Technol 8:576–582. https://doi.org/10.1361/105996399770350278

Goldbaum D, Manimuda P, Kamath G, Descartes S, Klemberg-Sapieha JE, Chromik RR (2016) Tribological behavior of TiN and Ti (Si,C)N coatings on cold sprayed Ti substrates. Surf Coat Technol 291:264–275. https://doi.org/10.1016/j.surfcoat.2016.02.044

Han T, Zhao Z, Gillispie BA, Smith JR (2005) Effects of spray conditions on coating formation by the kinetic spray process. J Therm Spray Technol 14:373–383. https://doi.org/10.1361/105996305X59369

Howe C (2014) Cold spray repair of the CH-47 accessory cover. In: CSAT Workshop. Worcester, USA

Howe C (2015) Cold spray qualification of T700 engine front frame. In: CSAT Workshop. Worcester, USA

Jakupi P, Keech PG, Barker I, Ramamurthy S, Jacklin RL, Shoesmith DW, Moser DE (2015) Characterization of commercially cold sprayed copper coatings and determination of the effects of impacting copper powder velocities. J Nucl Mater 466:1–11. https://doi.org/10.1016/j.jnucmat.2015.07.001

Jones R, Matthews N, Rodopoulos CA, Cairns K, Pitt S (2011) On the use of supersonic particle deposition to restore the structural integrity of damaged aircraft structures. Int J Fatigue 33:1257–1267. https://doi.org/10.1016/j.ijfatigue.2011.03.013

Jones R, Matthews N, Elston J, Cairns K, Baker J, Wadsley B, Pitt S (2012) SPD repairs to thin aluminium structures. In: 28th International Congress of the Aeronautical Sciences. Brisbane, Australia

Jones R, Molent L, Barter S, Matthews N, Tamboli D (2014) Supersonic particle deposition as a means for enhancing the structural integrity of aircraft structures. Int J Fatigue 68:260–268. https://doi.org/10.1016/j.ijfatigue.2014.03.013

Kashirin A, Klyuev O, Buzdygar T, Shkodkin A (2011) Modern applications of the low pressure cold spray. International Thermal Spray Conference, Hamburg

Kilchenstein G (2014) Cold spray technologies used for repair. In: JTEG Monthly Teleconference. http://jteg.ncms.org/wp-content/gallery/ColdSpray/ColdSpray_SlideDeck.pdf. Accessed 9 Nov 2016

Kotoban D, Grigoriev S, Okunkova A, Sova A (2016) Influence of a shape of single track on deposition efficiency of 316L stainless steel powder in cold spray. Surf Coat Technol. https://doi.org/10.1016/j.surfcoat.2016.10.052

Kumar S, Chavan NM (2011) Cold spray coating technology: activities at ARCI. International Advanced Reserch Centre for Powder Metallurgy and New Materials, Hyderabad

Lee JC, Kang HJ, Chu WS, Ahn SH (2007) Repair of damaged mold surface by cold-spray method. CIRP Ann – Manuf Technol 56:577–580. https://doi.org/10.1016/j.cirp.2007.05.138

Leyman PF, Champagne VK (2009) Cold spray process development for the reclamation of the Apache helicopter mast support. Report No.: ARL-TR-4922. Army Research Laboratory, MD, USA

Li CJ, Li WY, Wang YY, Yang GJ, Fukanuma H (2005) A theoretical model for prediction of deposition efficiency in cold spraying. Thin Solid Films 489:79–85. https://doi.org/10.1016/j.tsf.2005.05.002

Li CJ, Li WY, Liao H (2006) Examination of the critical velocity for deposition of particles in cold spraying. J Therm Spray Technol 15:212–222. https://doi.org/10.1361/105996306X108093

Li WY, Zhang C, Guo XP, Zhang G, Liao HL, Li CJ, Coddet C (2008) Effect of standoff distance on coating deposition characteristics in cold spraying. Materials and DesignMater Des 29:297–304. https://doi.org/10.1016/j.matdes.2007.02.005

Lu G, Lu GQ, Xiao ZM (1999) Mechanical properties of porous materials. J Porous Mater 6:359–368. https://doi.org/10.1023/A:1009669730778

Luo XT, Li YJ, Li CX, Yang GJ, Li CJ (2016) Effect of spray conditions on deposition behavior and microstructure of cold sprayed Ni coatings sprayed with a porous electrolytic Ni powder. Surf Coat Technol 289:85–93. https://doi.org/10.1016/j.surfcoat.2016.01.058

Lyalyakin VP, Kostukov AY, Denisov VA (2016) Special features of reconditioning the housing of a caterpillar diesel oil pump by gas-dynamic spraying. Weld Int 30:68–70. https://doi.org/10.1080/09507116.2015.1030152

MacDonald D, Fernández R, Delloro F, Jodoin B (2016) Cold spraying of Armstrong process titanium powder for additive manufacturing. J Therm Spray Technol. https://doi.org/10.1007/s11666-016-0489-2

Maev RG, Strumban E, Leshchinskiy V, Dzhurinskiy D (2014) Repair applications of the LPCS process. In: CSAT Workshop. Worcester, USA

Matthews N, Jones R, Sih GC (2014) Application of supersonic particle deposition to enhance the structural integrity of aircraft structures. Sci China Phys Mech Astron 57:12–18. https://doi.org/10.1007/s11433-013-5367-z

May C, Marx S, Paul A (2013) Selected R&D results and industrial applications. In: CSAT Workshop, Worcester, USA

Montevecchi F, Grossi N, Takagi H, Scippa A, Sasahara H, Campatelli G (2016) Cutting forces analysis in additive manufactured AISI H13 alloy. Procedia CIRP 46:476–479. https://doi.org/10.1016/j.procir.2016.04.034

Morgan R, Fox P, Pattison J, Sutcliffe C, O'Neill W (2004) Analysis of cold gas dynamically sprayed aluminium deposits. Mater Lett 58:1317–1320. https://doi.org/10.1016/j.matlet.2003.09.048

Moridi A, Hassani Gangaraj SM, Vezzu S, Guagliano M (2014) Number of passes and thickness effect on mechanical characteristics of cold spray coating. Procedia Eng 74:449–459. https://doi.org/10.1016/j.proeng.2014.06.296

Papyrin A (2001) Cold spray technology. Adv Mater Process 159:49–51

Pattison J, Celotto S, Morgan R, Bray M, O'Neill W (2007) Cold gas dynamic manufacturing: a non-thermal approach to freeform fabrication. Int J Mach Tools Manuf 47:627–634. https://doi.org/10.1016/j.ijmachtools.2006.05.001

Pattison J, Celotto S, Khan A, O'Neill W (2008) Standoff distance and bow shock phenomena in the cold spray process. Surf Coat Technol 202:1443–1454. https://doi.org/10.1016/j.surfcoat.2007.06.065

Ramulu M, Rao PN, Kao H (2002) Drilling of (Al_2O_3)p/6061 metal matrix composites. J Mater Process Technol 124:244–254. https://doi.org/10.1016/S0924-0136(02)00176-0

Rech S, Trentin A, Vezzù S, Vedelago E, Legoux JG, Irissou E (2014) Different cold spray deposition strategies: single- and multi-layers to repair aluminium alloy components. J Therm Spray Technol 6061:1237–1250. https://doi.org/10.1007/s11666-014-0141-y

Richter P (2014) New value chain for advanced coatings by using cold spray. In: Industrial Technologies 2014 – Smart Growth through Research and Innovation. Athens, Greece

Schell J (2016) Cold spray aerospace applications. In: CSAT Workshop, Worcester, USA

Security E, Program TC (2011) Cost and performance report cold spray for repair of magnesium. http://www.dtic.mil/dtic/tr/fulltext/u2/a572962.pdf. Accessed 28 Oct 2016

Sova A, Grigoriev S, Okunkova A, Smurov I (2013) Potential of cold gas dynamic spray as additive manufacturing technology. Int J Adv Manuf Technol 69:2269–2278. https://doi.org/10.1007/s00170-013-5166-8

Stier O (2014) Fundamental cost analysis of cold spray. J Therm Spray Technol 23:131–139. https://doi.org/10.1007/s11666-013-9972-1

Stoltenhoff T, Zimmermann F (2012) LOXPlate® coatings for aluminum aerospace components exposed to high dynamic stresses. Praxair Surface Technologies GmbH, Ratingen

Tabbara H, Gu S, McCartney DG, Price TS, Shipway PH (2011) Study on process optimization of cold gas spraying. J Therm Spray Technol 20:608–620. https://doi.org/10.1007/s11666-010-9564-2

Tutunea-Fatan OR, Fakhri MA, Bordatchev EV (2011) Porosity and cutting forces: from macroscale to microscale machining correlations. Proc Inst Mech Eng Part B J Eng Manuf 225:619–630. https://doi.org/10.1177/2041297510394057

Vilardell AM, Cinca N, Concustell A, Dosta S, Cano IG, Guilemany JM (2015) Cold spray as an emerging technology for biocompatible and antibacterial coatings: state of art. J Mater Sci 4441–4462. doi:https://doi.org/10.1007/s10853-015-9013-1

Villa M, Dosta S, Guilemany JM (2013) Optimization of 316L stainless steel coatings on light alloys using cold gas spray. Surf Coat Technol 235:220–225. https://doi.org/10.1016/j.surfcoat.2013.07.036

Villafuerte J (2015) Using cold spray to add features to components. http://www.coldsprayteam.com/files/Villafuerte%20CSAT%20using%20CS%20to%20add%20features.pdf. Accessed 27 Oct 2016

Widener CA, Carter MJ, Ozdemir OC, Hrabe RH, Hoiland B, Stamey TE, Champagne VK, Eden TJ (2016) Application of high-pressure cold spray for an internal bore repair of a navy valve actuator. J Therm Spray Technol 25:193–201. https://doi.org/10.1007/s11666-015-0366-4

Xiong Y, Zhuang W, Zhang M (2015) Effect of the thickness of cold sprayed aluminium alloy coating on the adhesive bond strength with an aluminium alloy substrate. Surf Coat Technol 270:259–265. https://doi.org/10.1016/j.surfcoat.2015.02.048

Yandouzi M, Gaydos S, Guo D, Ghelichi R, Jodoin B (2014) Aircraft skin restoration and evaluation. J Therm Spray Technol 23:1281–1290. https://doi.org/10.1007/s11666-014-0130-1

Yin S, Wang X, Li W, Liao H, Jie H (2012) Deformation behavior of the oxide film on the surface of cold sprayed powder particle. Appl Surf Sci 259:294–300. https://doi.org/10.1016/j.apsusc.2012.07.036

Yin S, Suo X, Su J, Guo Z, Liao H, Wang X (2013) Effects of substrate hardness and spray angle on the deposition behavior of cold-sprayed Ti particles. J Therm Spray Technol 23:76–83. https://doi.org/10.1007/s11666-013-0039-0

Yin S, Liu Q, Liao H, Wang X (2014) Effect of injection pressure on particle acceleration, dispersion and deposition in cold spray. Comput Mater Sci 90:7–15. https://doi.org/10.1016/j.commatsci.2014.03.055

Yin S, Suo X, Xie Y, Li W, Lupoi R, Liao H (2015) Effect of substrate temperature on interfacial bonding for cold spray of Ni onto cu. J Mater Sci 50:7448–7457. https://doi.org/10.1007/s10853-015-9304-6

Yin S, Xie Y, Cizek J, Ekoi E, Hussain T, Dowling D, Lupoi R (2017) Advanced diamond-reinforced metal matrix composites via cold spray: properties and deposition mechanism. Compos Part B Eng. https://doi.org/10.1016/j.compositesb.2017.01.009